

Federated Learning on Heterogeneous Data via Adaptive Self-Distillation

M Yashwanth, Gaurav Kumar Nayak, Arya Singh, Yogesh Simmhan, Anirban Chakraborty

Abstract—Federated Learning (FL) is a machine learning paradigm that enables clients to jointly train a global model by aggregating the locally trained models without sharing any local training data. In practice, there can often be substantial heterogeneity (e.g., class imbalance) across the local data distributions observed by each of these clients. Under such non-iid data distributions across clients, FL suffers from the ‘client-drift’ problem where every client converges to its own local optimum. This results in slower convergence and poor performance of the aggregated model. To address this limitation, we propose a novel regularization technique based on adaptive self-distillation (ASD) for training models on the client side. Our regularization scheme adaptively adjusts to the client’s training data based on: (i) the closeness of the local model’s predictions with that of the global model, and (ii) the client’s label distribution. The proposed regularization can be easily integrated atop existing, state-of-the-art FL algorithms leading to a further boost in the performance of these off-the-shelf methods. We demonstrate the efficacy of our proposed FL approach through extensive experiments on multiple real-world benchmarks (including datasets with common corruptions and perturbations) and show substantial gains in performance over the state-of-the-art methods. The code is provided in the supplementary.

Index Terms—Federated Learning, Knowledge Distillation, Heterogeneity & Generalization

I. INTRODUCTION

FEDERATED Learning (FL) is a machine learning method where the clients learn a shared model under the orchestration of the server without sharing the client’s data. Due to its privacy-preserving nature, it has many applications in smartphones [1], the Internet of Things (IoT), healthcare and insurance organizations [2], where training data is generated at edge devices or from privacy-sensitive domains. As originally introduced in [3], FL involves model training across an architecture consisting of one server and multiple clients. In traditional FL, each client securely holds its training data due to privacy concerns as well as to avoid large communication overheads while transmitting the same. At the same time, these clients aim to collaboratively train a generalized model that can leverage the entirety of the training data disjointly distributed across all these clients and thereby attain accuracy comparable to a centrally trained model.

One way to solve this problem is by FedSGD proposed by [3]. The problem with this approach is the communication

cost, as it takes a large number of rounds to converge. To minimize the communication cost and ensure faster convergence, they introduce the Federated Average (FedAvg) algorithm [3]. FedAvg shows excellent convergence when the data is independent and identically distributed (iid) or non-heterogeneous across the clients. But it has slower convergence and poor performance in non-iid or heterogeneous settings.

Data generated at the edge/client devices are often highly heterogeneous, as a consequence of the data generation process. They can differ in terms of quantity imbalance (the number of samples with each client), label imbalance (empirical label distribution across the clients), and feature imbalance (features of the data across the clients are non-iid). When there exists a label or feature imbalance, the objective for every client becomes different as the local minimum for every client will be different. In such settings, during the local training, the client’s model starts to drift towards its own local minimum and farther away from the global objective. This is undesirable as the goal of the FL is to converge to a global model that generalizes well across all the clients. This phenomenon, known as ‘client-drift’ is introduced and explored in earlier works [4], [5].

One popular way of mitigating this challenge of non-iid data distribution owing to label imbalance across clients is via client-side regularization. Here, the client models during local training are explicitly regularized with the global model parameters to minimize client drift. Algorithms such as FedProx [6], SCAFFOLD [4] and FedDyn [5] use regularization at the client-side in the parameter space. But they ignore the representations of the global model, which can be useful and are explored in distillation-based works in recent literature. Authors in [7] introduce the class-wise adaptive weighting scheme FedCAD at the server side. FedCAD relies on the server and the presence of auxiliary data for computing the class-wise weights. Another recent work [8] propose FedNTD by distilling only the incorrect class labels.

The primary motivation behind the distillation and regularization works in the context of FL is that the global model will have better representations than the local models. By introducing regularization on the client-side, we make the client models remain in proximity to the global model. This leads to faster convergence, i.e., obtaining the desired accuracy with minimum communication rounds. This is particularly helpful in FL where edge devices transmit and receive model parameters in each round, and this causes communication costs on the constrained edge devices [9].

Motivated by the utility of client model regularization in mitigating client drift we propose an efficient Adaptive Self

M. Yashwanth, Y. Simmhan, and A. Chakraborty are with the Department of Computational and Data Sciences, Indian Institute of Science, Bangalore, India.

G. K. Nayak is with the Centre for Research in Computer Vision, University of Central Florida, USA.

Arya is with the Birla Institute of Science and Technology, Goa, India.

For all correspondence: Anirban Chakraborty (anirban@iisc.ac.in)

Distillation (ASD) strategy for Federated learning. This is a distillation-based regularizer where the regularizer is adaptively adjusted based on the Kullback Leibler (KL) divergence between the global and local model predictions and the empirical label distribution of the client’s data. This novel design of our proposed ASD method can be easily integrated atop any existing FL methods to result in substantial performance gain, which makes it an attractive and compelling solution to the federated learning problem. To the best of our knowledge, this is the first work where the adaptive weights are used for the distillation loss in the FL framework without requiring access to auxiliary data and without the assistance of the server. As a validation, we combine our proposed regularization scheme with the algorithms such as FedAvg [3], FedProx [6], FedDyn [5] and FedNTD [8], and refer to the enhanced methods as FedAvg+ASD, FedProx+ASD, FedDyn+ASD and FedNTD+ASD respectively.

The key contributions of this work are, as follows.

- We introduced a novel regularization method ASD in the context of Federated Learning that alleviates the client drift problem by adaptively weighting the regularization loss for each sample based on two key factors: (i) closeness of predictions between the global model and the local model, and (ii) empirical label distribution of client data.
- Unlike prior works where regularization schemes are typically combined with the FedAvg algorithm, our proposed approach can be suitably combined with any state-of-the-art aggregation methods that further yields improvement in performance.
- We demonstrate the efficiency of our method by extensive experiments on CIFAR-10, CIFAR-100 and Tiny-ImageNet datasets to improve the accuracy and reduce the communication cost.
- We present the theoretical analysis of the client-drift and also the empirical evidence for better generalization ability of ASD.

II. RELATED WORK

A. Federated Learning (FL)

In recent times, addressing non-iid problems in Federated Learning has become an active area of research, and the field is developing rapidly. For brevity, we discuss a few related works here. In FedAvg [3], the two main challenges explored are reducing communication costs with fewer rounds and ensuring privacy by avoiding having to share the data. There are some studies based on gradient inversion [10] raising privacy concerns owing to gradient sharing while some studies have proposed in defense of sharing the gradients [11], [12].

FedAvg [3] is the generalization of local SGD [13] by increasing the number of local updates, significantly reducing communication costs for an iid setting, but does not give similar improvements for non-iid data. FedProx [6] introduced a proximal term by penalizing the weights if they are far from the global initialized model. SCAFFOLD [4] viewed this problem as one of objective inconsistency and introduced a gradient correction term which acts as a regularizer. Later,

FedDyn [5] improved upon this by introducing the dynamic regularization term. [14] attempts to solve this problem by enabling all device participation or none, as described by [5].

There are several papers that perform an SGD type analysis which involves the full device participation, and this breaks the important constraint in FL setup of partial device participation. Some of these attempt to compress the models to reduce the communication cost [15]. A few works include regularization methods on the client side [16], and one shot methods where clients send the condensed data and the server trains on the condensed data [17]. In [18], an adaptive weighting scheme is considered on task-specific loss to minimize the learning from samples whose representation is negligible.

B. Federated Learning using Knowledge Distillation

Knowledge Distillation (KD) introduced by [19] is a technique to transfer the knowledge from a pre-trained teacher model to the student model by matching the predicted probabilities. Adaptive distillation was used in [20]. The server-side KD methods such as FedGen [21] use KD to train the generator at the server and the generator is broadcasted to the clients in the subsequent round. The clients use the generator to generate the data to provide the inductive bias. This method incurs extra communication of generator parameters along the model and training of the generator in general is difficult. In FedDF [22] KD is used at the server that relies on the external data. The KD is performed on an ensemble of client models, especially client models act as a multiple Teacher models and the knowledge is distilled into a single student model, which is a global model. In FedNTD [8] the non-true class logits are used for distillation. This method gives uniform weight to all the samples. In FedCAD [7] and FedSSD [23] the client-drift problem is posed as a forgetting problem, and a weighting scheme has been proposed. Importantly, the weights are assisted by the server with the assumption that the server has access to auxiliary data. One shortcoming of this method is the availability of auxiliary data on the server, which may not hold. Unlike all of these approaches, we propose a novel adaptive distillation strategy that aims to mitigate the challenge of client drift due to non-iid data without relying on the server and access to any form of auxiliary data to compute the adaptive weights.

III. METHOD

We first describe the federated optimization problem in general, then explain the proposed method of adaptive self-distillation (ASD) in section III-B. We provide the theoretical and empirical analysis in the sections III-C and III-D respectively.

A. Problem Setup

We assume there is a single server/cloud and m clients/edge devices. We further assume that client k has the Dataset \mathcal{D}_k with n_k training samples drawn iid from the data distribution $\mathbb{P}_k(x, y)$. The data distributions $\{\mathbb{P}_k(x, y)\}_{k=1}^K$ across the

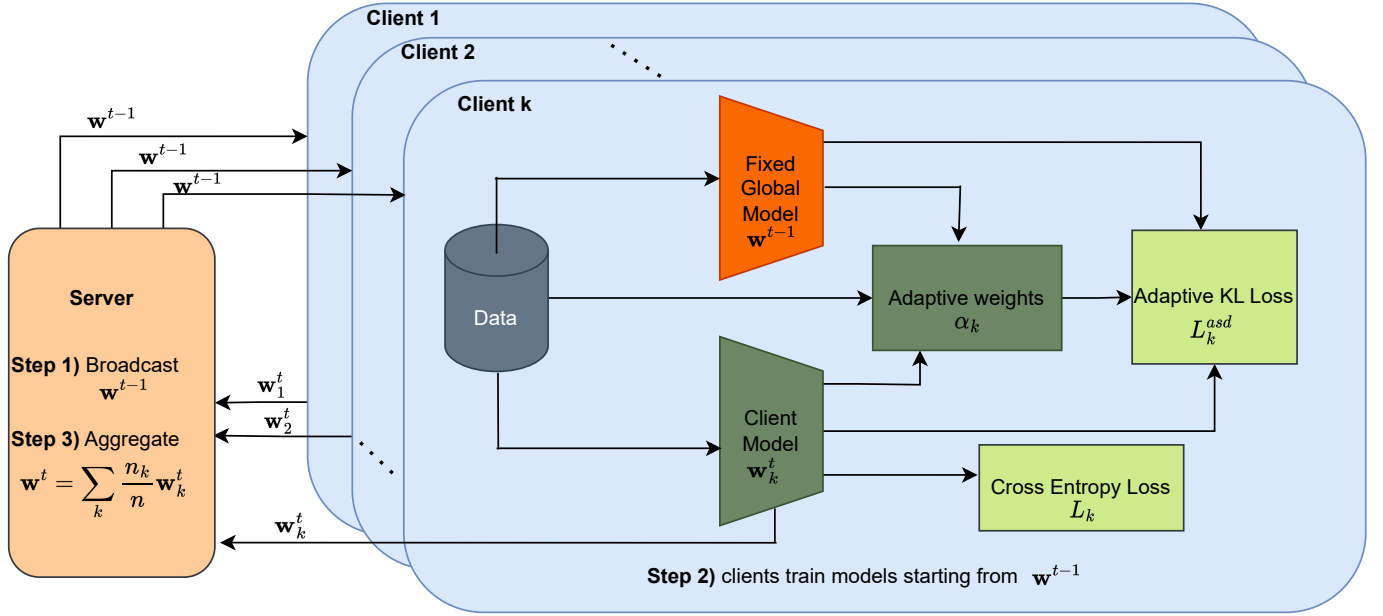


Fig. 1. Federated Learning with Adaptive Self Distillation: The figure describes the overview of the proposed approach based on Adaptive distillation. In **Step 1**, Server broadcasts the model parameters, In **Step 2**, clients train their models by minimizing both the cross entropy loss and predicted probability distribution over the classes between the global model and the client model by minimizing the KL divergence, the importance of the sample in the batch is decided by the proposed adaptive scheme as a function of label distribution and the KL term. The server model is fixed while training the client. In **Step 3**, Server aggregates the client models based on FedAvg aggregation. The process repeats till convergence.

clients are assumed to be non-iid. In this setup, we perform the following optimization. [5],[3]

$$\arg \min_{\mathbf{w} \in \mathbb{R}^d} \left(f(\mathbf{w}) \triangleq \frac{1}{K} \sum_{k \in [K]} f_k(\mathbf{w}) \right) \quad (1)$$

where $f_k(\mathbf{w})$ is the client specific objective function and w denotes model parameters. The overall FL framework is described in detail in figure 1.

B. Adaptive Self Distillation (ASD) in FL

We now describe the proposed method where each client k minimizes the $f_k(\mathbf{w})$ as defined below Eq. (2).

$$f_k(\mathbf{w}) \triangleq L_k(\mathbf{w}) + \lambda L_k^{asd}(\mathbf{w}) \quad (2)$$

$L_k(\mathbf{w})$ is given below.

$$L_k(\mathbf{w}) = \mathbb{E}_{x, y \in P_k(x, y)} [l_k(\mathbf{w}; (x, y))] \quad (3)$$

Here, l_k is cross-entropy loss. The expectation is computed over training samples drawn from $\mathbb{P}_k(x, y)$ of a client k . This is approximated as the empirical average of the samples from the Dataset \mathcal{D}_k .

$L_k^{asd}(\mathbf{w})$ in Eq. 2 denotes the proposed Adaptive Self Distillation loss (ASD) term which considers label imbalance and quantifies how easily the predictions of the local model can drift from the global model. ASD loss is designed so that client models learn from the local data at the same time not drift too much from the global model. We define (ASD) Loss as follows.

$$L_k^{asd}(\mathbf{w}) \triangleq \mathbb{E}[\alpha_k(x, y) \mathcal{D}_{\text{KL}}(q_g(x, \mathbf{w}^t) || q_k(x, \mathbf{w}))] \quad (4)$$

In the above Eq. 4 \mathbf{w}^t represents the global model at round t and \mathbf{w} represents the trainable model parameters of client k . $\alpha_k(x, y)$ denotes the weight for the sample x with label ground truth label y . For simplicity, we denote the global model softmax predictions $q_g(x, \mathbf{w}^t)$ as $q_g(x)$ and client model softmax predictions $q_k(x, \mathbf{w})$ as $q_k(x)$. \mathcal{D}_{KL} is the KL divergence. The Eq. 4 can be approximated by the below equation using the mini-batch.

$$L_k^{asd}(\mathbf{w}) = \frac{1}{B} \sum_{i \in [B]} \alpha_k(x^i, y^i) \mathcal{D}_{\text{KL}}(q_g(x^i) || q_k(x^i)) \quad (5)$$

where B is the batch size, $(x^i, y^i) \in \mathcal{D}_k$ and q_g and q_k are softmax probabilities on the temperature (τ) scaled logits of the global model and client model k respectively. They are given in Eq. 6 and Eq. 7.

$$q_g^c(x^i) = \frac{\exp(z_g^c(x^i)/\tau)}{\sum_{m \in \mathcal{C}} \exp(z_g^m(x^i)/\tau)} \quad (6)$$

$$q_k^c(x^i) = \frac{\exp(z_k^c(x^i)/\tau)}{\sum_{m \in \mathcal{C}} \exp(z_k^m(x^i)/\tau)} \quad (7)$$

where $z_g(x^i)$, $z_k(x^i)$ are the logits predicted on the input x^i by the global model and client model k respectively. The index i denotes the i^{th} sample of the batch. The $\mathcal{D}_{\text{KL}}(q_g(x^i) || q_k(x^i))$ is given in Eq. (8).

$$\mathcal{D}_{\text{KL}}(q_g(x^i) || q_k(x^i)) = \sum_{c=1}^{\mathcal{C}} q_g^c(x^i) \log(q_g^c(x^i)/q_k^c(x^i)) \quad (8)$$

where C is the number of classes. We use the simplified notation α_k^i for distillation weights $\alpha_k(x^i, y^i)$ and it is given in below Eq.9.

$$\alpha_k^i = \frac{\hat{\alpha}_k^i}{\sum_{i \in B} \hat{\alpha}_k^i} \quad (9)$$

and $\hat{\alpha}_k^i$ is defined as below Eq. 10

$$\hat{\alpha}_k^i \triangleq \exp(\beta^{kl} \mathcal{D}_{\text{KL}}(q_g(x^i) || q_k(x^i)) + \beta I(p_k^{y^i})) \quad (10)$$

where $\mathcal{D}_{\text{KL}}(q_g(x^i) || q_k(x^i))$ is given by (8). \mathcal{D}_{KL} term captures how close the local model's predictions are to the global model. If KL is high, then the samples are easy-to-drift. Our weighting scheme increases the weights when the KL term is high, forcing the easy-to-drift samples to stay close to the global model. The presence of the KL term will weigh every sample differently depending on how close it is to the global model.

The term $I(p_k^{y^i})$ defined as below.

$$I(p_k^{y^i}) \triangleq -\log(p_k^{y^i}) \quad (11)$$

where $p_k^{y^i}$ is the empirical label distribution, it is computed as Eq.12.

$$p_k^{y^i=c} = \frac{\sum_{i \in |\mathcal{D}_k|} \mathbb{1}_{y^i=c}}{|\mathcal{D}_k|} \quad (12)$$

where $\mathbb{1}_{y^i=c}$ denotes the indicator function and its value is 1 if the label of the i^{th} training sample y^i is class c else it is 0. $I(p_k^{y^i})$ term captures the label imbalance. Its value is higher when the probability of label is less; when the term $I(p_k^{y^i})$ is higher, the values of α_k^i are also higher, giving more weight to distillation loss. This term is specific to each client as the label distribution is unique to each client. This term ensures the client model predictions stay close to the global model if the samples belong to the class whose probability of occurrence is very low. To simplify notation, we use p_k^c for $p_k^{y^i=c}$ as it depends only on the class. The β and β^{kl} are the hyper-parameters, β captures how much importance will be given to label imbalance, and β^{kl} captures the importance given to KL term. Finally we use Eq.8, Eq.9 and Eq. 11 to compute the $L_k^{asd}(\mathbf{w})$ defined in Eq.5. The algorithm for combining ASD with FedAvg is given in Algorithm 1.

C. Theoretical Analysis

In this section, we perform the theoretical analysis of the client drift. We assume that $\beta^{kl} = 1$ and $\beta = 1$ in Eq. 10, which is also the default choice of hyper-parameters in our experiments. We now introduce the Gradient dissimilarity G_d based on the works of [6], [8] as a way to measure the extent of client-drift as below.

$$G_d(\mathbf{w}, \lambda) = \frac{\frac{1}{K} \sum_k \|\nabla f_k(\mathbf{w})\|^2}{\|\nabla f(\mathbf{w})\|^2} \quad (13)$$

$G_d(\mathbf{w}, \lambda)$ is function of both the \mathbf{w} and λ . For convenience, we simply write G_d and mention arguments when explicitly required. $f_k(\mathbf{w})$ in the above Eq. 13 is same as Eq. 2.

With this, we now establish a series of propositions to show

Algorithm 1 FedAvg+ASD

```

1: Server Executes
2: Initialize  $\mathbf{w}^t$ 
3: for every communication round  $t$  in  $T$  do
4:   sample random subset  $S$  of clients,  $S \subset [K]$ 
5:   for every client  $k$  in  $S$  in parallel do
6:      $\mathbf{w}_k^t = \mathbf{ClientUpdate}(k, \mathbf{w}^{t-1})$ 
7:   end for
8:    $\mathbf{w}^t = \mathbf{ServerAggregation}(\mathbf{w}_k^t)$ 
9: end for
10: procedure CLIENTUPDATE( $k, \mathbf{w}^{t-1}$ )
11:   set  $\mathbf{w}_k^t = \mathbf{w}^{t-1}$ 
12:   for every epoch  $e$  in  $E$  do
13:     for every batch  $b$  in  $B$  do
14:       Compute  $f_k(\mathbf{w})$  by computing  $\alpha_k, L_k$  &  $L_k^{asd}$ 
15:        $\mathbf{w}_k^t = \mathbf{w}_k^t - \nabla f_k(\mathbf{w}_k^t)$ 
16:     end for
17:   end for
18:   return  $\mathbf{w}_k^t$ 
19: end procedure
20: procedure SERVERAGGREGATION( $\mathbf{w}_k^t$ )
21:    $\mathbf{w}^t = \sum_k \frac{n_k}{n} \mathbf{w}_k^t$ 
22: end procedure

```

that ASD regularization reduces the client-drift as that leads to faster convergence.

Proposition 1: The minimum value gradient diversity G_d is 1 ($G_d \geq 1$). It is attained if all f_k are identical.

The above proposition implies that if all the client's gradients are progressing in the same direction, which means there is no drift $G_d = 1$. The result follows from Jensen's inequality, proof is provided in section 4 of supplementary material. The lower value of G_d is desirable and ideally 1. To analyze the G_d , we need $\nabla f_k(\mathbf{w})$ which is given in the below proposition.

Proposition 2: When the class conditional distribution across the clients is identical, i.e., $\mathbb{P}_k(x | y) = \mathbb{P}(x | y)$ then $\nabla f_k(\mathbf{w}) = \sum_c p_k^c (\mathbf{g}_c + \lambda \gamma_k^c \tilde{\mathbf{g}}_c)$, where $\mathbf{g}_c = \nabla \mathbb{E}[l(\mathbf{w}; x, y) | y = c]$, and $\tilde{\mathbf{g}}_c = \nabla \mathbb{E}[\exp(\mathcal{D}_{\text{KL}}(q_g(x) || q_k(x))) \mathcal{D}_{\text{KL}}(q_g(x) || q_k(x)) | y = c]$ where $\gamma_k^c = \frac{1}{p_k^c}$.

The result follows from the tower property of expectation and the assumption that class conditional distribution is the same for all the clients. From the above proposition, we can see that the gradients $\nabla f_k(\mathbf{w})$ only differ due to p_k^c which captures the data heterogeneity due to label imbalance. The detailed proof is given in section 4 of the supplementary.

Assumption 1: class-wise gradients are orthonormal $\mathbf{g}_c^T \mathbf{g}_m = 0$, $\tilde{\mathbf{g}}_c^T \tilde{\mathbf{g}}_m = 0$ and $\mathbf{g}_c^T \tilde{\mathbf{g}}_m = 0$ for $c \neq m$.

The assumption on orthonormal class-wise gradients intuitively implies that gradients of loss for a specific class cannot give any significant information on the gradients of the other class.

Proposition 3: When the class-conditional distribution across the clients is the same, and the Assumption 1 holds then \exists a range of values for λ such that whenever $\lambda \in (\lambda_{min}, \lambda_{max})$ we have $\frac{dG_d}{d\lambda} < 0$ and $G_d(\mathbf{w}, \lambda) < G_d(\mathbf{w}, 0)$.

The proposition implies that there is a value of $\lambda \in (\lambda_{min}, \lambda_{max})$ such that the derivative of G_d w.r.t λ is negative. The proof is given in section 4 of supplementary.

This indicates that by appropriately selecting the value of λ we can make the G_d lower which in turn reduces the client drift. This key result allows the ASD regularizer to combine with the existing methods and improve their performance.

To understand the convergence, we assume the following standard assumptions based on [4], [6].

Assumption 2: $\frac{1}{K} \sum_k \|\nabla f_k(\mathbf{w})\|^2 \leq B^2(\lambda) \|\nabla f(\mathbf{w})\|^2$

Assumption 3: $\|\nabla f_k(\mathbf{x}) - \nabla f_k(\mathbf{y})\| = \beta \|\mathbf{x} - \mathbf{y}\|$ (β smoothness)

Assumption 4: Gradients have bounded Variance.

Proposition 4: Suppose the functions f_k satisfy Assumption 2 above and $\mathbf{g}_c^T \mathbf{g}_c > 0$ then we have $B^2(\lambda) < B^2(0)$.

Proof: The Assumption 2 implies that $G_d(\mathbf{w}, \lambda) \leq B^2(\lambda)$, as $G_d(\mathbf{w}, \lambda)$ defined in Eq. 13. $B^2(\lambda)$ can be defined as below.

$$B^2(\lambda) = \sup_{\mathbf{w} \in \mathbb{R}^d} G_d(\mathbf{w}, \lambda) \quad (14)$$

For a fixed λ as per proposition 3 we have the following.

$$\sup_{\mathbf{w} \in \mathbb{R}^d} G_d(\mathbf{w}, \lambda) < \sup_{\mathbf{w} \in \mathbb{R}^d} G_d(\mathbf{w}, 0) \quad (15)$$

The above inequality 15 is true as proposition 3 guarantees that the value of $G_d(\mathbf{w}, \lambda) < G_d(\mathbf{w}, 0)$ for all \mathbf{w} when $\lambda \in (\lambda_{min}, \lambda_{max})$. If inequality 15 is not true, one can find a \mathbf{w} that contradicts the proposition 3 which is impossible. This means for some value of $\lambda \in (\lambda_{min}, \lambda_{max})$ we have $B^2(\lambda) < B^2(0)$ from Eq. 14 and Eq. 15. ■

To gain insights into the impact of the ASD regularizer on convergence, we further assume that functions L_k^{asd} in the Eq. 4 approximately constant in the argument \mathbf{w}^t . This allows us to treat f_k in Eq. 2 effectively as a function of \mathbf{w} . We can now use the convergence result from [4]. We state the result formally in the below proposition.

Proposition 5: Theorem V in [4]. Assume that $f(\mathbf{w})$ and $f_k(\mathbf{w})$, in our Eq. 1 satisfies Assumptions 2, 3 and 4. Let $\mathbf{w}^* = \arg \min f(\mathbf{w})$, the global step-size be α_g and the local step-size be α_l . FedAvg+ASD algorithm will have contracting gradients. If Initial model is \mathbf{w}^0 , $F = f(\mathbf{w}^0) - f(\mathbf{w}^*)$ and for constant M , then in R rounds, the model w^R satisfies $\mathbb{E}[\|\nabla f(\mathbf{w}^R)\|^2] \leq O(\frac{\beta M \sqrt{F}}{\sqrt{RLS}} + \frac{\beta B^2(\lambda) F}{R})$.

The above proposition gives the convergence rate for the FedAvg+ASD algorithm in the non-convex setting. We now show that FedAvg+ASD converges faster than FedAvg.

We see the convergence rate in proposition 5 is $O(\frac{\beta M \sqrt{F}}{\sqrt{RLS}} + \frac{\beta B^2(\lambda) F}{R})$. We can see that convergence has a direct dependence on $B^2(\lambda)$. This is the only term that is linked to heterogeneity assumption. So the lower value of $B(\lambda)$ implies faster convergence. From proposition 4 we have $B^2(\lambda) < B^2(0)$. Note that the case $\lambda = 0$ corresponds to without ASD. We have shown the tighter convergence for FedAvg+ASD. The key take away from the analysis is ASD helps in reducing the client-drift that leads to faster convergence.

D. Empirical Analysis

In the previous section we showed that when the clients use ASD loss, it will result in a lower value of G_d , and this in turn results in faster convergence for FedAvg+ASD compared to FedAvg. Since both FedAvg and FedAvg+ASD are optimizing different cost functions. It is natural to ask how well these solutions generalize to unseen data. We empirically observed that FedAvg+ASD generalizes much better than FedAvg. To better understand this phenomenon we consider analyzing the properties such as top eigenvalue and the trace of Hessian of the cross-entropy loss for the global models obtained with and without ASD. We follow the method described in [24] to compute the top eigenvalue and trace of the Hessian. In general, converging to the flat minima is indicative of better generalization this has been studied in [25] [24]. The lower values of the top eigenvalue and trace are typical indicators of the presence of flat minima. In the table I we can observe that FedAvg+ASD does achieve the lower value of top eigenvalue and trace compared to FedAvg, suggesting convergence to flat minima. We observe similar trends with FedNTD+ASD and FedDyn+ASD, the detailed results are presented in the section 3 of supplementary material.

TABLE I
HESSIAN ANALYSIS ON THE CONVERGED MODELS OBTAINED USING FEDAVG AND FEDAVG + ASD ON CIFAR-100 DATASET.

| Hessian Analysis | | |
|------------------|----------------|-------------|
| Method | Top Eigenvalue | Trace |
| FedAvg | 463 | 9500 |
| FedAvg + ASD | 23 | 1739 |

IV. EXPERIMENTS

We perform the experiments on CIFAR-10, CIFAR-100 dataset [26], Tiny-ImageNet [27] dataset, and the tailored version of CIFAR-100 dataset, with different degrees of heterogeneity in the balanced settings (i.e., the same number of samples per client but the class label distribution of each varies). We set the total number of clients to 100 in all our experiments. We sample the clients with a ratio of 0.1, i.e., 10 percent of clients are sampled on an average per communication round, similar to the protocol followed in [5]. We build our experiments using publicly available codebase by [5]. For generating non-iid data, Dirichlet distribution is used. To simulate the effect of label imbalance, for every client we sample the 'probability distribution' over the classes from the distribution $p_k^{dir} = Dir(\delta, C)$. Every sample of p_k^{dir} is a vector of length C and all the elements of this vector are non-negative and sum to 1. This vector represents the label distribution for the client. The parameter δ captures the degree of heterogeneity. Lower values of δ capture high heterogeneity and as the value of δ increases, the label distribution becomes more uniform. Another parameter of Dirichlet distribution (i.e., C), its value can be interpreted from the training dataset ($C = 100$ for CIFAR-100). For notational convenience, we omit C from $Dir(\delta, C)$ by simply re-writing as $Dir(\delta)$. By configuring the concentration parameter δ to 0.6 and 0.3, we

TABLE II

COMPARISON OF ACCURACY(%): WE SHOW THE ACCURACY ATTAINED BY THE ALGORITHMS ACROSS THE DATASETS (CIFAR-100/TINY-IMAGENET) AT THE END OF 500 COMMUNICATION ROUNDS. IT CAN BE SEEN THAT BY COMBINING THE PROPOSED APPROACH THE PERFORMANCE OF ALL THE ALGORITHMS IS IMPROVED. FEDDYN+ASD ATTAINS THE BEST PERFORMANCE WHEN COMPARED TO OTHER METHODS.

| Algorithm | CIFAR-100 | | | TinyImageNet | | |
|--------------------|-------------------------|-------------------------|-------------------------|--------------------------|-------------------------|-------------------------|
| | Non-IID | | IID | Non-IID | | IID |
| | $Dir(\delta = 0.3)$ | $Dir(\delta = 0.6)$ | | $Dir(\delta = 0.3)$ | $Dir(\delta = 0.6)$ | |
| FedAvg | 40.68 \pm 0.33 | 40.39 \pm 0.56 | 39.23 \pm 0.24 | 25.37 \pm (0.01) | 23.92 \pm 1.06 | 23.98 \pm 0.21 |
| FedAvg+ASD (Ours) | 43.75 \pm 0.11 | 43.51 \pm 0.63 | 43.56 \pm 0.22 | 26.0.8 \pm 0.42 | 25.89 \pm 0.19 | 25.79 \pm 0.11 |
| FedProx | 40.42 \pm 0.80 | 39.87 \pm 1.48 | 36.43 \pm 2.14 | 24.91 \pm (0.12) | 24.75 \pm 1.33 | 23.69 \pm 0.25 |
| FedProx+ASD (Ours) | 43.47 \pm 0.62 | 43.27 \pm 0.83 | 42.78 \pm 0.77 | 25.81 \pm 0.28 | 25.40 \pm 0.79 | 25.77 \pm 0.45 |
| FedNTD | 43.12 \pm 0.28 | 42.79 \pm 0.87 | 43.29 \pm 0.33 | 23.51 \pm 0.82 | 23.12 \pm 0.02 | 23.92 \pm 0.26 |
| FedNTD+ASD (Ours) | 44.93 \pm 0.32 | 44.83 \pm 0.49 | 43.71 \pm 0.36 | 26.42 \pm 0.12 | 25.15 \pm 0.39 | 24.46 \pm 0.42 |
| FedDyn | 49.38 \pm 0.46 | 49.89 \pm 0.41 | 50.24 \pm 0.31 | 28.54 \pm 0.49 | 29.33 \pm 0.3 | 29.59 \pm 0.31 |
| FedDyn+ASD (Ours) | 50.26 \pm 0.34 | 50.84 \pm 0.45 | 52.01 \pm 0.34 | 30.81 \pm 0.22 | 31.33 \pm 1.06 | 29.93 \pm 0.9 |

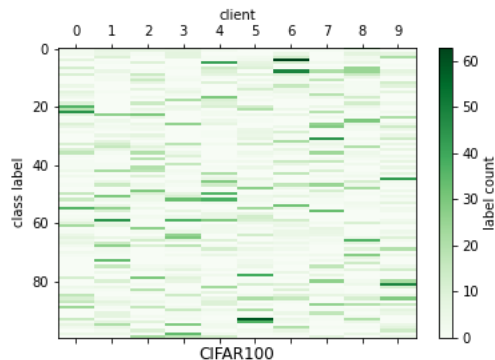


Fig. 2. Label distribution of clients: A subset containing 10 clients out of 100, and their corresponding label distribution based on Dirichlet distribution is plotted. It is easy to observe that the labels are not uniformly distributed across the clients.

generate the data from moderate to high heterogeneity, which is in line with the approach followed in [5] and [28]. In a balanced setting, each client receives the same number of samples. For instance, consider the case of CIFAR-100 where we have 50000 training samples. In the case of 100 clients, each client will get 500 samples, and the distribution of labels across the clients follows the Dirichlet distribution. Figure 2 shows the heatmap of the label distribution for a subset of 10 clients for the CIFAR-100 dataset.

V. RESULTS AND DISCUSSION

For evaluation, we report accuracy on the test dataset as our performance metric and the number of communication rounds required to attain the desired accuracy as a metric to quantify the communication cost. Specifically, we evaluate the global model on the test set and report its accuracy after every communication round. For comparison, we consider the popular methods for federated learning such as FedAvg [3], FedProx [6], FedDyn [5] and FedNTD [7]. We augment each of these methods with our approach (ASD) and observe a significant boost in performance. For a fair comparison, we consider the same models used in Fedavg [3], and FedDyn [5],

TABLE III

WE SHOW THE ACCURACY ATTAINED BY THE ALGORITHMS ON CIFAR-10 AT THE END OF 500 COMMUNICATION ROUNDS. IT CAN BE SEEN THAT BY COMBINING THE PROPOSED APPROACH THE PERFORMANCE OF ALL THE ALGORITHMS IS IMPROVED. FEDDYN+ASD ATTAINS THE BEST PERFORMANCE WHEN COMPARED TO OTHER METHODS.

| Algorithm | $Dir(\delta = 0.3)$ | $Dir(\delta = 0.6)$ | iid |
|--------------------|-------------------------|-------------------------|-------------------------|
| FedAvg | 79.27 \pm 0.20 | 80.0 \pm 0.08 | 81.47 \pm 0.27 |
| FedAvg+ASD (Ours) | 79.96 \pm 0.16 | 80.82 \pm 0.17 | 81.98 \pm 0.33 |
| FedProx | 79.75 \pm 0.26 | 80.15 \pm 0.17 | 81.4 \pm 0.37 |
| FedProx+ASD (Ours) | 80.21 \pm 0.25 | 80.75 \pm 0.27 | 81.96 \pm 0.36 |
| FedNTD | 78.97 \pm 0.34 | 79.77 \pm 0.22 | 81.04 \pm 0.06 |
| FedNTD+ASD (Ours) | 79.62 \pm 0.18 | 80.42 \pm 0.09 | 81.34 \pm 0.14 |
| FedDyn | 81.85 \pm 0.33 | 82.49 \pm 0.15 | 83.77 \pm 0.15 |
| FedDyn+ASD (Ours) | 82.61 \pm 0.06 | 83.27 \pm 0.07 | 84.40 \pm 0.09 |

for CIFAR-10 and CIFAR-100 classification tasks. The model architecture used for CIFAR-100 contains 2 convolution layers followed by 3 fully connected layers. For Tiny-ImageNet, we use 3 convolution followed by 3 fully connected layers. The detailed architectures are given in supplementary material.

Unlike existing works, we further evaluate our proposed method in extreme non-IID conditions. To mimic such scenarios, we create a corrupted version of CIFAR-100 with different levels of noise based on [29] and name it CIFAR-100C. The impulse noise is added to the CIFAR-100 dataset with five levels of severity. The first 10K samples are noise-free, the next 10K at increased severity, further next 10K at even more severity, and so on. Overall, we create a total of 50000 training samples where the noise increases from the first 10k samples being noise-free to the last 10k samples being heavily corrupted.

In this work, we use the proposed approach ASD with FedAvg, FedProx, FedDyn and FedNTD and refer to them as FedAvg+ASD, FedProx+ASD, FedDyn+ASD and FedNTD+ASD respectively.

Hyper-parameters: SGD algorithm with a learning rate of 0.1 and the decay learning rate per round of 0.998 is used to train the client models. Temperature τ is set to 2.0. We only tune the hyper-parameter λ . The β , and β^{kl} are always set to 1 and the value of λ is set to 20 and 30 for CIFAR-100 and Tiny-

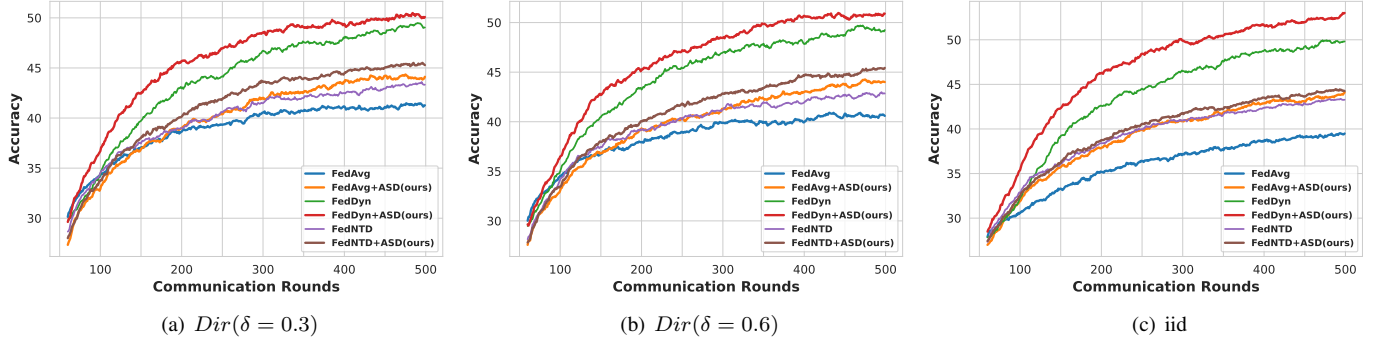


Fig. 3. Test Accuracy vs Communication rounds: Comparison of algorithms with $Dir(\delta = 0.3)$, $Dir(\delta = 0.6)$ and iid data partitions on CIFAR-100 dataset. All the algorithms augmented with proposed regularization (ASD) outperform compared to their original form. FedDyn+ASD outperforms all the other algorithms.

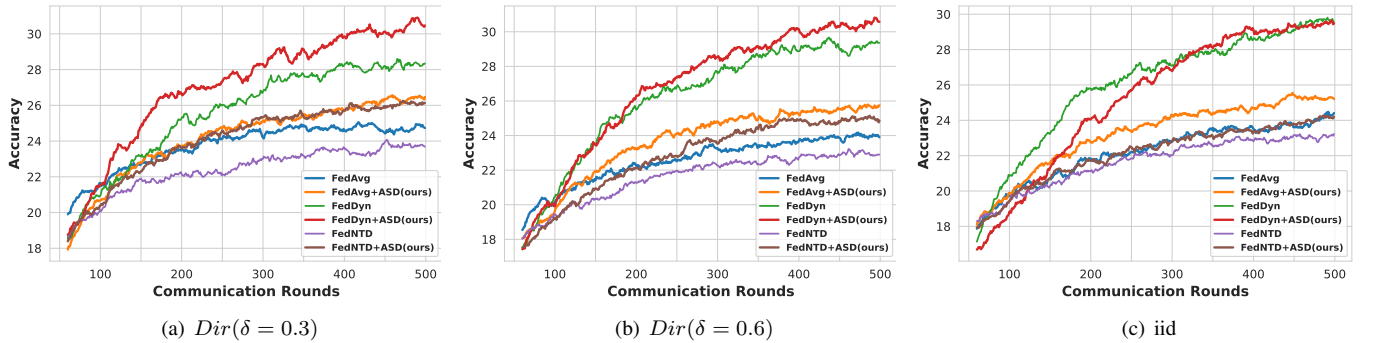


Fig. 4. Test Accuracy vs Communication rounds: Comparison of algorithms with $Dir(\delta = 0.3)$, $Dir(\delta = 0.6)$ and iid data partitions on Tiny-ImageNet dataset. All the algorithms augmented with proposed regularization (ASD) outperform compared to their original form. FedDyn+ASD outperforms all the other algorithms, except iid case where it performs close to FedDyn

ImageNet respectively for all our experiments. We compare the convergence of different schemes for 500 communication rounds. Following the testing protocol of [5], we average across all the client models and compute the test accuracy on the averaged model, which is reported in our results. In all the tables, we report the test accuracy of the global model in % at the end of 500 communication rounds. All the experiments in the Tables are performed over three different initializations, mean and standard deviations of accuracy over the three experiments are reported. In the figures 3 and 4 we report the test accuracy after every communication round.

A. Performance of ASD on CIFAR-10, CIFAR-100 and Tiny-ImageNet

In Table II, we report the performance of CIFAR-100 and Tiny-ImageNet datasets with various algorithms for non-iid ($Dir(\delta = 0.3)$ and $Dir(\delta = 0.6)$) and the iid settings. We observe that our proposed ASD applied on FedDyn improves its performance by $\approx 1.0\%$ for $Dir(\delta = 0.3)$ and $Dir(\delta = 0.6)$. The accuracy vs communication rounds plots is shown in Figure 3, we can see that adding ASD gives consistent improvement across the rounds¹. For the Tiny-

¹In the figures we omit the comparison between FedProx and FedProx+ASD for better readability.

ImageNet dataset, we observe that FedDyn+ASD improves FedDyn by $\approx 2\%$ for $Dir(\delta = 0.3)$ and $Dir(\delta = 0.6)$ and almost similar in the iid partition. The improvement in the iid case for Tiny-ImageNet dataset is marginal because we did not tune the hyper-parameter λ for every experiment, intuitively the lower value of λ will be better for iid case. The test accuracy vs communication rounds plot on Tiny-ImageNet are shown in Figure 4. We obtain significant improvements for FedAvg+ASD against FedAvg, FedProx+ASD against FedProx and for FedNTD+ASD against FedNTD. In the Table III we present the CIFAR-10 results, we observe that adding ASD consistently gives an improvement of $\approx 0.7\% - 0.8\%$ improvement across all the algorithms.

B. Analyzing the Communication cost

In this section, we analyze the communication cost (i.e., the number of communication rounds) for attaining a specified accuracy. From Table IV, we can infer that in all data heterogeneity settings across the datasets, the federated learning algorithms when augmented with the proposed regularizer outperform its original implementation. In particular, FedDyn+ASD outperforms all the algorithms. For attaining 26% accuracy with $Dir(\delta = 0.3)$ on the Tiny-ImageNet dataset, FedDyn+ASD takes 169 rounds while FedDyn takes 242

TABLE IV

COMPARISON OF COMMUNICATION ROUNDS TO ATTAIN SPECIFIC ACCURACY: WE SHOW THE NUMBER OF COMMUNICATION ROUNDS REQUIRED TO ATTAIN THE SPECIFIED ACCURACY CIFAR-100 = 40% AND TINYIMAGENET = 26%.

| Algorithm | CIFAR-100 | | | TinyImageNet | | |
|-------------------|---------------------|---------------------|------------|---------------------|---------------------|------------|
| | Non-IID | | IID | Non-IID | | IID |
| | $Dir(\delta = 0.3)$ | $Dir(\delta = 0.6)$ | | $Dir(\delta = 0.3)$ | $Dir(\delta = 0.6)$ | |
| FedAvg | 282 | 308 | 500+ | 500+ | 500+ | 500+ |
| FedAvg+ASD(ours) | 237 | 231 | 254 | 416 | 500+ | 500+ |
| FedProx | 330 | 362 | 500+ | 500+ | 500+ | 500+ |
| FedProx+ASD(ours) | 244 | 242 | 254 | 500+ | 500+ | 500+ |
| FedNTD | 238 | 239 | 246 | 500+ | 500+ | 500+ |
| FedNTD+ASD(ours) | 196 | 199 | 235 | 406 | 500+ | 500+ |
| FedDyn | 153 | 144 | 159 | 242 | 209 | 219 |
| FedDyn+ASD(ours) | 122 | 123 | 130 | 169 | 196 | 256 |

rounds. Similarly, the FedNTD+ASD needs 406 rounds while FedNTD takes 500+ rounds saving at least 92 rounds of communication cost.

TABLE V

CIFAR-100C ACCURACY WITH $Dir(\delta = 0.3)$. FEDDYN+ASD PERFORMS BETTER THAN OTHER ALGORITHMS

| Algorithm | CIFAR-100C |
|--------------------|-------------------------|
| FedAvg | 36.24 \pm 0.34 |
| FedAvg+ASD (ours) | 38.58 \pm 0.79 |
| FedProx | 36.29 \pm 0.71 |
| FedProx+ASD (ours) | 38.66 \pm 0.42 |
| FedNTD | 38.10 \pm 0.6 |
| FedNTD+ASD (ours) | 39.97 \pm 0.72 |
| FedDyn | 43.18 \pm 0.37 |
| FedDyn+ASD (ours) | 44.73 \pm 0.13 |

C. Efficacy of ASD in extreme non-IID cases

In Table V, we analyze the performance of federated learning algorithms for the extreme non-IID case (CIFAR-100C). We observe that our proposed FedDyn with ASD performs 1.40% better than FedDyn. FedNTD+ASD improves FedNTD by 2.43%. Similarly, FedAvg+ASD improves FedAvg by 2.79%. Hence, our method ASD yields consistent gains even in extreme non-IID settings.

D. Sensitivity to hyper parameters λ

We study the impact of changing the hyper-parameter on the CIFAR-100 dataset with the non-iid partition of $Dir(\delta = 0.3)$. When using FedAvg+ASD algorithm, the only hyper-parameter we consider is λ , the other parameters β and β^{kl} are kept to 1. In Figure 5 we see that the accuracy of the model increases with λ and then drops after a critical point. Overall the accuracy varies from 42.75% to 44.5% and doesn't drastically impact the accuracy.

E. Impact of \mathcal{D}_{KL} and the $I(p_k^{y^i})$

We analyze the contribution of KL term for FedAvg+ASD algorithm on the CIFAR-100 dataset with $Dir(\delta = 0.3)$ non-iid data partition. In table VI, we analyze the contribution

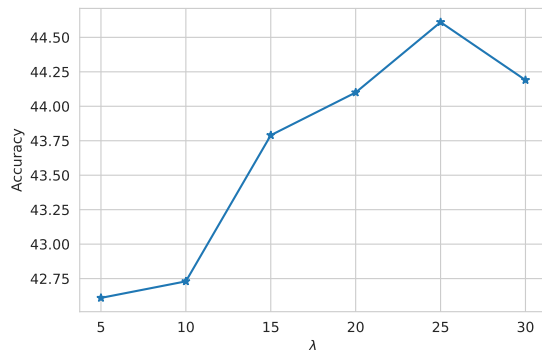


Fig. 5. Study of hyper-parameter's sensitivity for CIFAR100 and $Dir(\delta = 0.3)$ with FedAvg+ASD. Accuracy is sensitive at lower values of λ .

of each term by setting the hyperparameter β and β^{kl} for CIFAR-100 and CIFAR-100C. It can be seen that both the β and β^{kl} significantly contribute, and when both are used, it further leads to improved performance. All the accuracies are reported by averaging over three different initializations.

TABLE VI

ABLATION STUDY ON CIFAR-100 AND CIFAR-100C DATASETS

| Algorithm | β | β^{kl} | Accuracy CIFAR-100 | Accuracy CIFAR-100C |
|------------|---------|--------------|--------------------|---------------------|
| FedAvg | NA | NA | 40.68 \pm 0.33 | 36.24 \pm 0.34 |
| FedAvg+ASD | 1 | 0 | 43.33 \pm 0.56 | 38.22 \pm 0.53 |
| FedAvg+ASD | 0 | 1 | 43.10 \pm 0.22 | 37.20 \pm 0.22 |
| FedAvg+ASD | 1 | 1 | 43.75 \pm 0.11 | 38.58 \pm 0.79 |

F. Comparison with adaptive vs uniform weights

We analyze the impact of the proposed adaptive weighting scheme. We compare by making all the alpha values in Eq 10 to 1. This can be obtained by setting the values of β and β^{kl} to 0. We can see from Table VII that in the non-iid scenarios, the proposed adaptive weighting scheme is better than assigning the uniform weights, thus establishing the impact of proposed adaptive weights. In iid cases, it impacts very marginally.

TABLE VII
COMPARISON WITH ADAPTIVE WEIGHTS VS UNIFORM WEIGHTS ON
CIFAR-100 DATASET

| Data partition | Self Distillation with Uniform weights | Self Distillation with Adaptive weights |
|-------------------------------|---|--|
| | $\beta = 0, \beta^{kl} = 0$ | $\beta = 1, \beta^{kl} = 1$ |
| <i>Dir</i> ($\delta = 0.3$) | 41.81 \pm 0.52 | 43.75 \pm 0.11 |
| <i>Dir</i> ($\delta = 0.6$) | 42.53 \pm 0.11 | 43.51 \pm 0.63 |
| IID | 43.86 \pm 0.05 | 43.56 \pm 0.22 |

VI. COMPUTATION COST

In this section we quantify the amount of computation increased in the proposed method vs the accuracy benefits obtained. As described in [30] the major computational burden for the distillation scheme comes from the teacher forward pass, student forward pass and the student backward pass. Let F_t , F_s and B_s denote the number of operations for teacher forward pass, student forward pass and student backward pass respectively. Overall cost with batch of N_b samples given below.

$$C_{reg} = (F_t + F_s + B_s) * N_b \quad (16)$$

$$C_{noreg} = (F_s + B_s) * N_b \quad (17)$$

C_{reg} is the cost due to the proposed regularization cost and C_{noreg} is the cost without regularization. It can be clearly seen that we increase the computation cost per batch due to the teacher model by $N_b * F_t$. The cost is linear in batch size and since we use the same model architecture for student and teacher we have $F_t = F_s$ this implies we double the forward pass computation. If storing the model is too expensive then one can get all the predictions, i.e., the softmax probabilities and store them instead of the model. This way one can save the memory and the repeated computations of the global model.

VII. PRIVACY OF PROPOSED METHOD

In our method, which is ASD regularizer, the adaptive weights are computed by the client without depending on the server and it does not assume access to any auxiliary data at the server as assumed in methods such as FedCAD [7] and FedDF [22]. In our method, only model parameters are communicated with the server similar to FedAvg [3]. Thus our privacy is similar to the FedAvg method at the same time obtaining significant improvements in the performance.

VIII. CONCLUSION

We presented an efficient and effective method for addressing data heterogeneity due to label imbalance in Federated learning using Adaptive Self Distillation (ASD), which does not require any auxiliary data and no extra communication cost. We also theoretically showed that ASD has lower client-drift leading to better convergence. Moreover, we also performed empirical analysis to show that ASD has better generalization by analyzing Hessian's top eigenvalue and trace. The effectiveness of our approach is shown via extensive experiments across datasets such as CIFAR-10, CIFAR-100 and Tiny-ImageNet with different degrees of heterogeneity. Our proposed approach ASD can be integrated easily into any

of the FL frameworks. We showed its efficacy by improving the performance when combined with FedAvg, FedDyn, and FedNTD. We also observed that our method achieves flat minima on convergence. As a future investigation, we aim to look into a deeper theoretical analysis of ASD.

REFERENCES

- [1] A. Hard, C. M. Kiddon, D. Ramage, F. Beaufays, H. Eichner, K. Rao, R. Mathews, and S. Augenstein, "Federated learning for mobile keyboard prediction," 2018. [Online]. Available: <https://arxiv.org/abs/1811.03604>
- [2] N. Rieke, J. Hancox, W. Li, F. Milletari, H. R. Roth, S. Albarqouni, S. Bakas, M. N. Galtier, B. A. Landman, K. Maier-Hein *et al.*, "The future of digital health with federated learning," *NPJ digital medicine*, vol. 3, no. 1, pp. 1–7, 2020.
- [3] B. McMahan, E. Moore, D. Ramage, S. Hampson, and B. A. y Arcas, "Communication-efficient learning of deep networks from decentralized data," in *Artificial intelligence and statistics*. PMLR, 2017, pp. 1273–1282.
- [4] S. P. Karimireddy, S. Kale, M. Mohri, S. Reddi, S. Stich, and A. T. Suresh, "Scaffold: Stochastic controlled averaging for federated learning," in *International Conference on Machine Learning*. PMLR, 2020, pp. 5132–5143.
- [5] D. A. E. Acar, Y. Zhao, R. M. Navarro, M. Mattina, P. N. Whatmough, and V. Saligrama, "Federated learning based on dynamic regularization," *arXiv preprint arXiv:2111.04263*, 2021.
- [6] T. Li, A. K. Sahu, M. Zaheer, M. Sanjabi, A. Talwalkar, and V. Smith, "Federated optimization in heterogeneous networks," *Proceedings of Machine Learning and Systems*, vol. 2, pp. 429–450, 2020.
- [7] Y. He, Y. Chen, X. Yang, Y. Zhang, and B. Zeng, "Class-wise adaptive self distillation for heterogeneous federated learning," 2022.
- [8] G. Lee, M. Jeong, Y. Shin, S. Bae, and S.-Y. Yun, "Preservation of the global knowledge by not-true distillation in federated learning," in *Advances in Neural Information Processing Systems*, A. H. Oh, A. Agarwal, D. Belgrave, and K. Cho, Eds., 2022. [Online]. Available: <https://openreview.net/forum?id=qw3MZb1Juo>
- [9] S. Yadav and R. S. Yadav, "A review on energy efficient protocols in wireless sensor networks," *Wireless Networks*, vol. 22, no. 1, pp. 335–350, 2016.
- [10] J. Geiping, H. Bauermeister, H. Dröge, and M. Moeller, "Inverting gradients-how easy is it to break privacy in federated learning?" *Advances in Neural Information Processing Systems*, vol. 33, pp. 16937–16947, 2020.
- [11] P. Kairouz, H. B. McMahan, B. Avent, A. Bellet, M. Bennis, A. N. Bhagoji, K. Bonawitz, Z. Charles, G. Cormode, R. Cummings *et al.*, "Advances and open problems in federated learning," *Foundations and Trends® in Machine Learning*, vol. 14, no. 1–2, pp. 1–210, 2021.
- [12] Y. Huang, S. Gupta, Z. Song, K. Li, and S. Arora, "Evaluating gradient inversion attacks and defenses in federated learning," *Advances in Neural Information Processing Systems*, vol. 34, pp. 7232–7241, 2021.
- [13] S. U. Stich, "Local sgd converges fast and communicates little," *arXiv preprint arXiv:1805.09767*, 2018.
- [14] X. Zhang, M. Hong, S. Dhople, W. Yin, and Y. Liu, "Fedpd: A federated learning framework with optimal rates and adaptivity to non-iid data," *arXiv preprint arXiv:2005.11418*, 2020.
- [15] K. Mishchenko, E. Gorbunov, M. Takáč, and P. Richtárik, "Distributed learning with compressed gradient differences," *arXiv preprint arXiv:1901.09269*, 2019.
- [16] Z. Zhu, J. Hong, and J. Zhou, "Data-free knowledge distillation for heterogeneous federated learning," in *International Conference on Machine Learning*. PMLR, 2021, pp. 12878–12889.
- [17] Y. Zhou, G. Pu, X. Ma, X. Li, and D. Wu, "Distilled one-shot federated learning," *arXiv preprint arXiv:2009.07999*, 2020.
- [18] T.-M. H. Hsu, H. Qi, and M. Brown, "Federated visual classification with real-world data distribution," in *Computer Vision—ECCV 2020: 16th European Conference, Glasgow, UK, August 23–28, 2020, Proceedings, Part X 16*. Springer, 2020, pp. 76–92.
- [19] G. Hinton, O. Vinyals, J. Dean *et al.*, "Distilling the knowledge in a neural network," *arXiv preprint arXiv:1503.02531*, vol. 2, no. 7, 2015.
- [20] S. Tang, L. Feng, W. Shao, Z. Kuang, W. Zhang, and Y. Chen, "Learning efficient detector with semi-supervised adaptive distillation," *arXiv preprint arXiv:1901.00366*, 2019.

- [21] H. Seo, J. Park, S. Oh, M. Bennis, and S.-L. Kim, "16 federated knowledge distillation," *Machine Learning and Wireless Communications*, p. 457, 2022.
- [22] T. Lin, L. Kong, S. U. Stich, and M. Jaggi, "Ensemble distillation for robust model fusion in federated learning," *Advances in Neural Information Processing Systems*, vol. 33, pp. 2351–2363, 2020.
- [23] Y. He, Y. Chen, X. Yang, H. Yu, Y.-H. Huang, and Y. Gu, "Learning critically: Selective self-distillation in federated learning on non-iid data," *IEEE Transactions on Big Data*, pp. 1–12, 2022.
- [24] Z. Yao, A. Gholami, K. Keutzer, and M. W. Mahoney, "Pyhessian: Neural networks through the lens of the hessian," in *2020 IEEE international conference on big data (Big data)*. IEEE, 2020, pp. 581–590.
- [25] N. S. Keskar, D. Mudigere, J. Nocedal, M. Smelyanskiy, and P. T. P. Tang, "On large-batch training for deep learning: Generalization gap and sharp minima," in *International Conference on Learning Representations*, 2017. [Online]. Available: <https://openreview.net/forum?id=H1oyRIYgg>
- [26] A. Krizhevsky and G. Hinton, "Learning multiple layers of features from tiny images," Canadian Institute for Advanced Research, Tech. Rep., 2009.
- [27] Y. Le and X. Yang, "Tiny imagenet visual recognition challenge," *CS 231N*, vol. 7, no. 7, p. 3, 2015.
- [28] M. Yurochkin, M. Agarwal, S. Ghosh, K. Greenwald, N. Hoang, and Y. Khazaeni, "Bayesian nonparametric federated learning of neural networks," in *International Conference on Machine Learning*. PMLR, 2019, pp. 7252–7261.
- [29] D. Hendrycks and T. Dietterich, "Benchmarking neural network robustness to common corruptions and perturbations," *Proceedings of the International Conference on Learning Representations*, 2019.
- [30] G. Xu, Z. Liu, and C. C. Loy, "Computation-efficient knowledge distillation via uncertainty-aware mixup," *arXiv preprint arXiv:2012.09413*, 2020.

Supplementary for “Federated Learning on Heterogeneous Data via Adaptive Self-Distillation”

I. MODEL ARCHITECTURES

In Table I, the model architecture is shown. We use PyTorch style representation. For example conv layer(3,64,5) means 3 input channels, 64 output channels and the kernel size is 5. Maxpool(2,2) represents the kernel size of 2 and a stride of 2. FullyConnected(384,200) represents an input dimension of 384 and an output dimension of 200. The architecture for CIFAR-100 is exactly the same as used in [5].

| CIFAR-100 Model | Tiny ImageNet Model | |
|--------------------------|----------------------------|--------------------|
| | | ConvLayer(3,64,3) |
| | | GroupNorm(4,64) |
| | | Relu |
| | | MaxPool(2,2) |
| | | ConvLayer(64,64,3) |
| | GroupNorm(4,64) | |
| ConvLayer(3,64,5) | Relu | |
| Relu | MaxPool(2,2) | |
| MaxPool(2,2) | ConvLayer(64,64,3) | |
| ConvLayer(64,64,5) | GroupNorm(4,64) | |
| Relu | Relu | |
| MaxPool(2,2) | MaxPool(2,2) | |
| Flatten | Flatten | |
| FullyConnected(1600,384) | FullyConnected(4096,512) | |
| Relu | Relu | |
| FullyConnected(384,192) | FullyConnected(512,384) | |
| Relu | Relu | |
| FullyConnected(192,100) | FullyConnected(384,200) | |

TABLE I

MODELS USED FOR TINY IMAGENET AND CIFAR-100 DATASETS.

II. HYPER-PARAMETER SETTINGS

We summarize the hyper-parameter settings in the Table II

TABLE II
HYPERPARAMETER SETTINGS

| DataSet | λ | β | β^{kl} |
|--------------|-----------|---------|--------------|
| CIFAR-10 | 1 | 1 | 1 |
| CIFAR-100 | 20 | 1 | 1 |
| TinyImageNet | 30 | 1 | 1 |

III. HESSIAN ANALYSIS

TABLE III

THE TABLE SHOWS THE IMPACT OF ASD ON THE FEDAVG, FEDDYN AND FEDNTD ALGORITHMS. WE CONSISTENTLY SEE THAT THE TOP EIGENVALUE AND THE TRACE OF THE HESSIAN DECREASE AND THE ACCURACY IMPROVES WHEN ASD IS USED. THIS SUGGESTS THAT USING ASD MAKES THE GLOBAL MODEL REACH TO A FLAT MINIMUM FOR BETTER GENERALIZATION.

| Algorithm | CIFAR-100 | | | Tiny-ImageNet | | |
|------------|----------------|----------------|--------------|----------------|----------------|--------------|
| | Top eigenvalue | Trace | Accuracy | Top eigenvalue | Trace | Accuracy |
| FedAvg | 463.51 | 9500.04 | 41.27 | 140.85 | 10661.8 | 24.75 |
| FedAvg+ASD | 23.59 | 1739.53 | 44.12 | 16.78 | 2609.31 | 26.47 |
| FedNTD | 74.4 | 2474.34 | 43.33 | 40.07 | 3567.98 | 23.68 |
| FedNTD+ASD | 43.81 | 2128.17 | 45.28 | 26.75 | 2323.51 | 26.13 |
| FedDyn | 440.13 | 7710.42 | 49.04 | 125.91 | 9015.98 | 28.35 |
| FedDyn+ASD | 19.96 | 2800.44 | 50.09 | 19.96 | 2800.44 | 30.47 |

In the Table III we analyze the top eigenvalue and the trace of the Hessian for all the algorithms. We observe that when ASD is used with the algorithms, it consistently improves the accuracy and reduces the top eigenvalue and the trace of the Hessian, this implies that ASD helps in converging to the flat minima which is a typical indicator of better generalization. We consider the CIFAR-100 and Tiny-ImageNet datasets with non-iid partition of $Dir(\delta = 0.3)$.

IV. PROOFS OF PROPOSITIONS:

We rewrite the adaptive weighting equations for convenience as below.

$$\hat{\alpha}_k^i \triangleq \exp(\beta^{kl} \mathcal{D}_{\text{KL}}(q_g(x^i) || q_k(x^i)) + \beta I(p_k^y)) \quad (1)$$

$$\alpha_i^k = \frac{\hat{\alpha}_i^k}{\sum_{i \in B} \hat{\alpha}_i^k} \quad (2)$$

Proposition 6: The minimum value gradient diversity G_d is 1 ($G_d \geq 1$). It is attained if all f_k are identical.

Proof:

$$G_d = \frac{\frac{1}{K} \sum_k \|\nabla f_k\|^2}{\|\nabla f\|^2} \quad (3)$$

$$\|\nabla f\|^2 = \left\| \frac{1}{K} \sum_k \nabla f_k \right\|^2 \quad (4)$$

Apply Jenson's inequality we get the desired result.

$$\|\nabla f\|^2 \leq \frac{1}{K} \sum_k \|\nabla f_k\|^2 \quad (5)$$

Lemma 1: For any function of the form $\zeta(x) = \frac{a_n x^2 + b x + c_n}{a_d x^2 + b x + c_d}$ satisfying $a_n < a_d$, $c_n < c_d \exists x \geq 0$ such that $\frac{d\zeta(x)}{dx} < 0 \forall x \in (x_{\min}, x_{\max})$ ■

Proof:

$$\frac{d\zeta(x)}{dx} = \frac{(2a_n x + b)(a_d x^2 + b x + c_d) - (2a_d x + b)(a_n x^2 + b x + c_n)}{(a_d x^2 + b x + c_d)^2} \quad (6)$$

By re-arranging and simplifying the above we get the following

$$\frac{d\zeta(x)}{dx} = \frac{b(a_n - a_d)x^2 + 2x(a_n c_d - a_d c_n) + b(c_d - c_n)}{(a_d x^2 + b x + c_d)^2} \quad (7)$$

Lets us call the numerator in the above equation as $\eta(x) = b(a_n - a_d)x^2 + 2x(a_n c_d - a_d c_n) + b(c_d - c_n)$. We are interested in knowing when $\eta(x) < 0$.

We now analyze the two cases $b < 0$ and $b > 0$ separately.

Case 1: ($b > 0$)

As $\eta(x)$ is a simple quadratic in x , we observe that the coefficient of x^2 , i.e., $b(a_n - a_d) < 0$ by assumptions, and the discriminant Δ is given as.

$$\Delta = 4(a_n c_d - a_d c_n)^2 - 4b^2(a_n - a_d)(c_d - c_n) \quad (8)$$

We observe that $\Delta > 0$ as $(a_n - a_d)(c_d - c_n) < 0$ by assumptions. This implies that $\eta(x)$ has two real roots and the fact that $\eta(0) > 0$, there must exist a positive root x_c such that $\eta(x) < 0$ whenever $x > x_c$. This concludes the proof.

Case 2: ($b < 0$)

We observe that the coefficient of x^2 i.e., $b(a_n - a_d) > 0$ by assumptions, and the discriminant Δ is given in Eq. 8. We observe that $\Delta > 0$. This implies that $\eta(x)$ has two real roots and the fact that $\eta(0) < 0$, there must exist a positive root x_c such that $\eta(x) < 0$ whenever $x < x_c$.

This concludes the proof. ■

Proposition 7: When the class conditional distribution across the clients is identical, i.e., $\mathbb{P}_k(x | y) = \mathbb{P}(x | y)$ then $\nabla f_k(\mathbf{w}) = \sum_c p_k^c(\mathbf{g}_c + \lambda \gamma_k^c \tilde{\mathbf{g}}_c)$, where $\mathbf{g}_c = \nabla \mathbb{E}[l(\mathbf{w}; x, y) | y = c]$, and $\tilde{\mathbf{g}}_c = \nabla \mathbb{E}[\exp(\mathcal{D}_{\text{KL}}(q_g(x) || q_k(x))) \mathcal{D}_{\text{KL}}(q_g(x) || q_k(x)) | y = c]$ and $\gamma_k^c = \frac{1}{p_k^c}$.

Proof: We re-write the equations for $f_k(\mathbf{w})$ from Sec 3.3 of main paper, $L_k(\mathbf{w})$ and $L_k^{asd}(\mathbf{w})$ from the Sec 3.2 of main paper for convenience.

$$f_k(\mathbf{w}) = L_k(\mathbf{w}) + \lambda L_k^{asd}(\mathbf{w}) \quad (9)$$

$$L_k(\mathbf{w}) = \mathbb{E}_{x, y \in D_k} [l_k(\mathbf{w}; (x, y))] \quad (10)$$

$$L_k^{asd}(\mathbf{w}) \triangleq \mathbb{E}[\alpha_k(x, y) \mathcal{D}_{\text{KL}}(q_g(x) || q_k(x))] \quad (11)$$

By applying the tower property of expectation, we expand Eq. 10 as below

$$L_k(\mathbf{w}) = \sum_c p_k^c \mathbb{E}[l_k(\mathbf{w}; x, y) \mid y = c] \quad (12)$$

If we assume the class-conditional distribution across the clients to be identical the value of $\mathbb{E}[l_k(\mathbf{w}; x, y) \mid y = c]$ is same for all the clients. Under such assumptions, we can drop the client index k and rewrite the Eq. 12 as follows

$$L_k(\mathbf{w}) = \sum_c p_k^c \mathbb{E}[l(\mathbf{w}; x, y) \mid y = c] \quad (13)$$

$$\nabla L_k(\mathbf{w}) = \sum_c p_k^c \nabla \mathbb{E}[l(\mathbf{w}; x, y) \mid y = c] \quad (14)$$

We further simplify the notation by denoting $\mathbf{g}_c = \nabla \mathbb{E}[l(\mathbf{w}; x, y) \mid y = c]$.

$$\nabla L_k(\mathbf{w}) = \sum_c p_k^c \mathbf{g}_c \quad (15)$$

To make the analysis tractable, In Eq. 1 we assume the value of β^{kl} to be 1 and β to be 1, and we use the un-normalized weighting scheme as the constant can be absorbed into λ . we can re-write Eq. 1 as below

$$\hat{\alpha}_k^i = \gamma_k^y \exp(\mathcal{D}_{\text{KL}}(q_g(x) \parallel q_k(x))) \quad (16)$$

where $\gamma_k^y = \frac{1}{p_k^y}$ With the above assumptions we can interpret the Eq. 11 as follows.

$$L_k^{asd} = \mathbb{E}_{x, y \in D_k} [l_k^{dist}(\mathbf{w}; (x, y))] \quad (17)$$

where $l_k^{dist}(\mathbf{w}; (x, y)) = \gamma_k^y \exp(\mathcal{D}_{\text{KL}}(q_g(x) \parallel q_k(x))) \mathcal{D}_{\text{KL}}(q_g(x) \parallel q_k(x))$.

By following the similar line of arguments from Eq. 12 to Eq. 14 we can write the following

$$\nabla L_k^{asd}(\mathbf{w}) = \sum_c p_k^c \tilde{\mathbf{g}}_c \gamma_k^c \quad (18)$$

$$\nabla f_k(\mathbf{w}) = \sum_c p_k^c (\mathbf{g}_c + \lambda \gamma_k^c \tilde{\mathbf{g}}_c) \quad (19)$$

Lemma 2: If $c_n = \sum_{k=1}^K \sum_{c=1}^C (p_k^c)^2$, $c_d = \sum_{k=1}^K \sum_{k2=1}^K \sum_{c=1}^C (p_{k1}^c p_{k2}^c)$, $a_n = KC$ and $a_d = K^2C$. where $p_k^c \geq 0 \forall k, c$, and $\sum_{c=1}^C p_k^c = 1$, then $\frac{c_n}{c_d} \geq \frac{a_n}{a_d}$.

Proof: We need to show that

$$\frac{\sum_{k=1}^K \sum_{c=1}^C (p_k^c)^2}{\sum_{k1=1}^K \sum_{k2=1}^K \sum_{c=1}^C (p_{k1}^c p_{k2}^c)} \geq \frac{1}{K} \quad (20)$$

By rewriting the denominator we get

$$\frac{\sum_{k=1}^K \sum_{c=1}^C (p_k^c)^2}{\sum_{c=1}^C (\sum_{k=1}^K (p_k^c))^2} \geq \frac{1}{K} \quad (21)$$

Consider rewriting the denominator of the L.H.S of above equation.

$$\sum_{c=1}^C (\sum_{k=1}^K (p_k^c))^2 = \sum_{c=1}^C ((\mathbf{p}^c)^\top \mathbf{1})^2 \quad (22)$$

where $\mathbf{p}^c = [p_1^c p_2^c \dots p_K^c]^\top$ and $\mathbf{1}$ is the all one vector of size K

Applying the Cauchy Schwartz inequality to the R.H.S of the Eq. 22 we get the following.

$$\sum_{c=1}^C ((\mathbf{p}^c)^\top \mathbf{1})^2 \leq \sum_{c=1}^C \sum_{k=1}^K (p_k^c)^2 K \quad (23)$$

By combining the Eq. 22 and Eq. 23 the result follows. ■

Proposition 8: When the class-conditional distribution across the clients is same and the class-wise gradients are orthogonal $\mathbf{g}_c^\top \mathbf{g}_k = 0$, $\tilde{\mathbf{g}}_c^\top \tilde{\mathbf{g}}_k = 0$ and $\mathbf{g}_c^\top \tilde{\mathbf{g}}_k = 0$ then \exists a range of values for λ such that whenever $\lambda \in (\lambda_{min}, \lambda_{max})$ we have $\frac{dG_d}{d\lambda} < 0$ and $G_d(\mathbf{w}, \lambda) < G_d(\mathbf{w}, 0)$

Proof:

$$G_d = \frac{\frac{1}{K} \sum_{k=1}^K \|\nabla f_k\|^2}{\|\nabla f\|^2} \quad (24)$$

From the Sec 3.2 of the main paper we have the following, We drop the argument \mathbf{w} for the functions f_k to simplify the notation

$$\nabla f_k = \sum_{c=1}^C p_k^c (g_c + \lambda \gamma_k^c \tilde{g}_c) \quad (25)$$

$$\begin{aligned} \|\nabla f_k\|^2 &= \sum_{c1=1}^C \sum_{c2=1}^C p_k^{c1} p_k^{c2} (\mathbf{g}_{c1}^T + \lambda \gamma_k^{c1} \tilde{\mathbf{g}}_{c1}^T) (\mathbf{g}_{c2} + \lambda \gamma_k^{c2} \tilde{\mathbf{g}}_{c2}) \\ &= \sum_{c1=1}^C \sum_{c2=1}^C p_k^{c1} p_k^{c2} (\mathbf{g}_{c1}^T \mathbf{g}_{c2} + \lambda \gamma_k^{c2} \mathbf{g}_{c1}^T \tilde{\mathbf{g}}_{c2} + \lambda \gamma_k^{c1} \tilde{\mathbf{g}}_{c1}^T \mathbf{g}_{c2} + \lambda^2 \gamma_k^{c2} \gamma_k^{c1} \tilde{\mathbf{g}}_{c1}^T \tilde{\mathbf{g}}_{c2}) \\ &= \sum_{c=1}^C (p_k^c)^2 (\mathbf{g}_c^T \mathbf{g}_c + \lambda \gamma_k^c \mathbf{g}_c^T \tilde{\mathbf{g}}_c + \lambda \gamma_k^c \tilde{\mathbf{g}}_c^T \mathbf{g}_c + \lambda^2 \gamma_k^c \gamma_k^c \tilde{\mathbf{g}}_c^T \tilde{\mathbf{g}}_c) \\ &= \sum_{c=1}^C (p_k^c)^2 (1 + 2\lambda \gamma_k^c \mathbf{g}_c^T \tilde{\mathbf{g}}_c + \lambda^2 (\gamma_k^c)^2) \\ &= \sum_{c=1}^C (p_k^c)^2 + 2\lambda \sum_{c=1}^C (p_k^c \mathbf{g}_c^T \tilde{\mathbf{g}}_c) + \lambda^2 C \end{aligned} \quad (26)$$

In the above equation the second equality is obtained by simply expanding the product, the third by orthonormal assumption of the gradients. The last two equalities used the fact that $\gamma_k^c = \frac{1}{p_k^c}$.

Finally we have the following

$$\begin{aligned} \frac{1}{K} \sum_{k=1}^K \|\nabla f_k\|^2 &= \frac{1}{K} \left(\sum_{k=1}^K \sum_{c=1}^C (p_k^c)^2 + 2\lambda \sum_{k=1}^K \sum_{c=1}^C p_k^c \mathbf{g}_c^T \tilde{\mathbf{g}}_c + \lambda^2 KC \right) \\ &= \frac{1}{K} (a_n \lambda^2 + b\lambda + c_n) \end{aligned} \quad (27)$$

where

$$a_n := KC \quad (28)$$

$$b := 2 \sum_{k=1}^K \sum_{c=1}^C p_k^c \mathbf{g}_c^T \tilde{\mathbf{g}}_c$$

$$c_n := \sum_{k=1}^K \sum_{c=1}^C (p_k^c)^2 \quad (29)$$

$$\begin{aligned} \|\nabla f\|^2 &= \left(\left\| \frac{1}{K} \sum_{k=1}^K \sum_{c=1}^C p_k^c (\mathbf{g}_c + \lambda \gamma_k^c \tilde{\mathbf{g}}_c) \right\| \right)^2 \\ &= \frac{1}{K^2} \sum_{k1=1}^K \sum_{k2=1}^K \sum_{c1=1}^C \sum_{c2=1}^C p_{k1}^{c1} (\mathbf{g}_{c1}^T + \lambda \gamma_{k1}^{c1} \tilde{\mathbf{g}}_{c1}^T) p_{k2}^{c2} (\mathbf{g}_{c2} + \lambda \gamma_{k2}^{c2} \tilde{\mathbf{g}}_{c2}) \\ &= \frac{1}{K^2} \sum_{k1=1}^K \sum_{k2=1}^K \sum_{c=1}^C p_{k1}^c p_{k2}^c (\mathbf{g}_c^T \mathbf{g}_c + \lambda \gamma_{k1}^c \mathbf{g}_c^T \tilde{\mathbf{g}}_c + \lambda \gamma_{k2}^c \tilde{\mathbf{g}}_c^T \mathbf{g}_c + \lambda^2 \gamma_{k1}^c \gamma_{k2}^c \tilde{\mathbf{g}}_c^T \tilde{\mathbf{g}}_c) \\ &= \frac{1}{K^2} \sum_{k1=1}^K \sum_{k2=1}^K \sum_{c=1}^C (p_{k1}^c p_{k2}^c + \lambda p_{k2}^c \mathbf{g}_c^T \tilde{\mathbf{g}}_c + \lambda p_{k1}^c \tilde{\mathbf{g}}_c^T \mathbf{g}_c + \lambda^2) \\ &= \frac{1}{K^2} \left(\sum_{k1=1}^K \sum_{k2=1}^K \sum_{c=1}^C (p_{k1}^c p_{k2}^c) + 2\lambda \sum_{k=1}^K \sum_{c=1}^C p_k^c \mathbf{g}_c^T \tilde{\mathbf{g}}_c + \lambda^2 K^2 C \right) \\ &= \frac{1}{K^2} (a_d \lambda^2 + b\lambda + c_d) \end{aligned} \quad (30)$$

By defining

$$a_d := K^2 C \quad (31)$$

$$c_d := \sum_{k_1=1}^K \sum_{k_2=1}^K \sum_{c=1}^C (p_{k_1}^c p_{k_2}^c) \quad (32)$$

By substituting Eq. 27 and Eq. 30 in Eq. 24 we get

$$G_d(\mathbf{w}, \lambda) = K \frac{a_n \lambda^2 + b\lambda + c_n}{a_d \lambda^2 + b\lambda + c_d} \quad (33)$$

Comparing Eq. 28 and Eq. 31 we see that $a_n < a_d$. Similarly by comparing Eq. 29 and Eq. IV we see that $c_n < c_d$. From Lemma 2 We have $\frac{c_n}{c_d} \geq \frac{a_n}{a_d}$.

We are interested in the values of λ for which $G_d(\mathbf{w}, \lambda) < G_d(\mathbf{w}, 0)$. Solving for λ we get the following inequality

$$\lambda > \frac{b(c_d - c_n)}{a_d c_n - a_n c_d} \quad (34)$$

We analyze the two cases when $b > 0$ and $b < 0$ separately.

Case1: ($b > 0$). Consider rewriting the Eq. 33 as below

$$G_d(\mathbf{w}, \lambda) = K \eta(\lambda) \quad (35)$$

where

$$\eta(\lambda) := \frac{\lambda^2 a_n + b\lambda + c_n}{\lambda^2 a_d + b\lambda + c_d} \quad (36)$$

As $K > 0$, it is enough to know when $\frac{d\eta(x)}{dx} < 0$. Using the Lemma 1 for $\eta(\lambda)$ when $b > 0$, We have a value of λ_c such that if $\lambda > \lambda_c$ $\frac{d\eta(x)}{dx} < 0$. by chosing the value of $\lambda > \max(\lambda_c, \frac{b(c_d - c_n)}{a_d c_n - a_n c_d})$ we can see that the value of $G_d(\mathbf{w}, \lambda) < G_d(\mathbf{w}, 0)$ and $G_d(\mathbf{w}, \lambda)$ decreases as λ increases.

We can attain the value of $G_d(\mathbf{w}, \lambda) = 1$ by increasing λ to infinity. This however has the down-side as very high values of λ restrict the local learning which results in very small gradient updates which is undesired.

Case2: ($b < 0$). Again Applying the Lemma 1 to $\eta(\lambda)$ when $b < 0$ we get the value of λ_c such that whenever $\lambda < \lambda_c$ the value of $G_d(\mathbf{w}, \lambda) < G_d(\mathbf{w}, 0)$ and $G_d(\mathbf{w}, \lambda)$ decreases when $\lambda \in (0, \lambda_c)$.

This concludes the proof. ■

V. COMBINING ASD WITH FED-NTD [8] AND FED-DYN [5]

A. Fed-Dyn with ASD

The algorithm for FedDyn is given in Algorithm 2. We use the Eq.1 of main paper as the client loss $f_k(\mathbf{w})$, which is the sum of the cross-entropy loss and the proposed adaptive self-distillation loss.

B. Fed-NTD with ASD

FedNTD [8] uses the non-true distillation loss, it distills the knowledge only from the non-true classes.

$$\mathcal{D}_{\text{NTD}}(q_g(x^i) || q_k(x^i)) = \sum_{c \neq y}^C q_g^c(x^i) \log(q_g^c(x^i) / q_k^c(x^i)) \quad (37)$$

The above equation represents the FedNTD loss on the sample i , when the true class label is y . We now use the adaptive weights as defined in Eq. 2, to update the FedNTD loss as below.

$$L_k^{\text{asd-ntd}}(\mathbf{w}) \triangleq \sum_{i \in [B]} \alpha_i^k \mathcal{D}_{\text{NTD}}(q_g(x^i) || q_k(x^i)) \quad (38)$$

So the final loss used for optimizing FedNTD with adaptive self-distillation is given below

$$f_k(\mathbf{w}) \triangleq L_k(\mathbf{w}) + \lambda L_k^{\text{asd-ntd}}(\mathbf{w}) \quad (39)$$

Algorithm 2 FedDyn [5] with ASD (FedDyn+ASD)

```

1: Input  $T, \mathbf{w}^0, \alpha, \nabla f_k(\mathbf{w}_k^0) = \mathbf{0}$ 
2: Initialize  $\mathbf{w}^t$ 
3: for every communication round  $t$  in  $T$  do
4:   sample random subset  $S$  of clients,  $S \subset [K]$ 
5:   for every client  $k$  in  $S$  in parallel do
6:      $w_t^k = \text{ClientUpdate}(k, w_{t-1})$ 
7:   end for
8:    $w_t = \text{ServerAggregation}(w_t^k)$ 
9: end for
10: procedure CLIENTUPDATE( $k, w_{t-1}$ )
11:   set  $\mathbf{w}_k^t = \arg \min_{\mathbf{w}} f_k(\mathbf{w}) - \langle \nabla f_k(\mathbf{w}_k^{t-1}), \mathbf{w} \rangle + \frac{\alpha}{2} \|\mathbf{w} - \mathbf{w}^{t-1}\|^2$ 
12:   set  $\nabla f_k(\mathbf{w}_k^t) = \nabla f_k(\mathbf{w}_k^{t-1}) - \alpha(\mathbf{w}_k^t - \mathbf{w}^{t-1})$ 
13:   return  $w_t^k$ 
14: end procedure
15: procedure SERVERUPDATE( $k, w_{t-1}$ )
16:   set  $\mathbf{h}^t = \mathbf{h}^{t-1} - \frac{\alpha}{m} (\sum_{k \in S} \mathbf{w}_k^t - \mathbf{w}^{t-1})$ 
17:   set  $\mathbf{w}^t = \frac{1}{|S|} (\sum_{k \in S} \mathbf{w}_k^t - \frac{1}{\alpha} \mathbf{h}^t)$ 
18:   return  $\mathbf{w}_t$ 
19: end procedure

```

where $L_k(\mathbf{w})$ is defined as in Eq.3 of the main paper. The α_k^i is defined in below Eq. 40.

$$\alpha_k^i = \frac{\hat{\alpha}_k^i}{\sum_{i \in B} \hat{\alpha}_k^i} \quad (40)$$

and the $\hat{\alpha}_k^i$ is defined in below Eq. 41

$$\hat{\alpha}_k^i \triangleq \exp(\beta^{kl} \mathcal{D}_{\text{NTD}}(q_g(x^i) || q_k(x^i)) + \beta I(p_k^{y^i})) \quad (41)$$